Analysis of LLC resonant converter performance with PIDD2 controller for electric vehicle application

Sathya K., K. P. Guruswamy
Department of Electrical Engineering, University Visvesvaraya College of Engineering (UVCE),
Bangalore, India

Article Info

Article history:

Received Jun 28, 2024
Revised Sep 23, 2024
Accepted Sep 30, 2024

Keywords:

LLC resonant converter
MATLAB/Simulink
PFM
PID
PIDD2

ABSTRACT

The key uses of the latest developments is electric vehicles (EV's). As a result, several researchers were drawn to EV's control to propose appropriate controllers and predicted that control engineers face a challenge when it comes to regulating the LLC resonant converter output voltage. In this regard, the study proposes a PID Type modified controller for regulation of voltage across output in LLC resonant converter. The design and control procedure of this modified proportional integral derivative double derivative (PIDD2) is explained along with EDF modeling in LLC resonant converter. This work proposes to use two controllers to drive the voltage output of a resonant converter LLC to constantly track the desired value. Proportional integral derivative controller (PID) is the first, while the PIDD2 method is the foundation of the second. Every controller has undergone simulation testing and the results are compared based on how the evaluated controllers respond dynamically in accordance with settling time, rising time and overshoot.

Corresponding Author:

Sathya K.
Department of Electrical Engineering, University Visvesvaraya College of Engineering (UVCE)
Bengaluru, India
Email: sathya.k@uvce.ac.in

1. INTRODUCTION

Conventional fossil fuels such as coal, oil, and natural gas have been the main source of continuous economic expansion for most industrial sectors. But using fossil fuels has resulted in emissions of CO_2, the main culprit behind climate change. The long-term effects of toxic emissions from gasoline and diesel cars are detrimental to public health. Both the business and academic sectors are paying increasing attention to clean energy technology and zero-carbon cars as solutions to the energy and environmental issues. Hence the transportation sector is transitioning from conventional internal combustion engine vehicles (ICVs) to electric vehicles (EVs) as a result of the depletion of fossil fuels and the rise in alternative energy sources. In the automobile industry, EVs are starting to lead the way. A sufficient quantity of charging stations with numerous chargers, little to no wait periods for charging, quick charging capabilities, and increased range are all necessary for the mainstream adoption of EVs. High-power chargers are necessary to enable electric automobiles to charge rapidly and significantly increase their driving range.

The resonant LLC converter architecture has shown to be a successful method for generating the necessary isolated DC/DC converter stage, as these high-power chargers now need to be separated from the grid. LLC resonant converter attributes such as high-power density, low noise and high efficiency, it is utilized in wide applications, inclusive of electric vehicles [1], power electronics [2], renewable energy, micro grids [3], uninterrupted power supply, DC motor drivers, telecommunications, battery chargers, and switch mode power supplies. The LLC resonant converters are often modulated using pulse frequency modulation (PFM) and a wide range of switching frequencies are generally required for a range of input voltages [2], [4], [5]. An LLC resonant converter with a zero-voltage switching (ZVS) system can achieve greater conversion efficiency by allowing its active switches to open and close. It is challenging to analyze and regulate this resonant converter optimally, which results in large errors and extended processing times. The output voltage of LLC resonant converter is controlled using several traditional methods including PID, PI, and PD. and have the benefits of being inexpensive as well as simple to use [6]. But they also need a sophisticated mathematical model and are unable to guarantee the intended performance under different operating situations [7], [8]. Furthermore, the literature review indicates that researchers have been drawn to the stability analysis and controller design issues of LLC resonant converters, which has led to improvements in transient domain specifications even in the face of multiple uncertainties and perturbations.

The research focused on controller design in this paper, specifically using the PIDD2 [9] control design to address the LLC resonant converter voltage control issue. Several control design techniques for LLC resonant converters have been described by researchers in the literature. However, it is depicted from the survey that is done that the PIDD2 controller has not been investigated for LLC resonant converter voltage regulation. This research paper presents the proposed PIDD2 approach to calibrate the LLC resonant converter output voltage value to the reference voltage value. PIDD2 controllers provide accurate control of the LLC converter using minimal rise time, overshoot, and settling time. Following the presentation of PIDD2 and PID simulation results, a comparison analysis of the two controllers under consideration is done. Additionally, with sudden changes in input voltage and load, the effectiveness and efficiency of the PIDD2 controller are examined. The findings from the simulation are compared with each other.

2. MODELING AND DESIGN OF LLC RESONANT CONVERTER

As illustrated in the Figure 1, LLC resonant converter is composed of two switches (MOSFET), four diodes, a high frequency transformer and an LLC filter. In order to maintain a fixed duty cycle of 50%, the complementary power switches Q1 and Q2 frequency is managed by the frequency controlled switching network, which also serves as a square wave generator [1], [4]. The resonant tank receives this square wave, the current passing through the network consists of transformer's magnetizing inductance L_m, the resonant capacitance C_r, and the series resonant inductance L_r make up the resonant circuit with a turn ratio of n supplying and circulating energy to the load. The specifications of inductors and capacitors are estimated, wide supply voltage range and switching frequency are key components in design [10], [11].

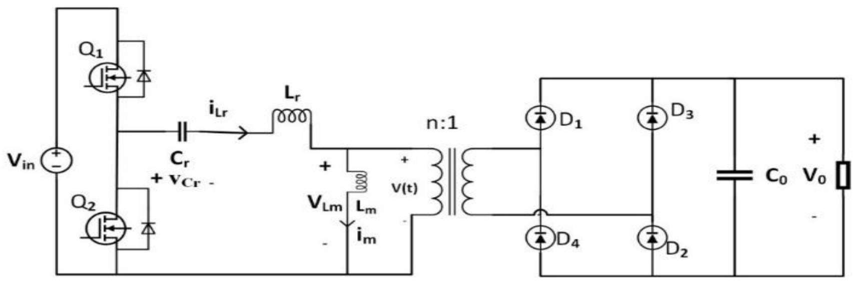

Figure 1. LLC resonant converter schematic

Circuit parameters are computed using the pertinent equations for developing LLC resonant converters [12]. The converter operates at 12 volts, with a switching frequency (F_s) of 80 kHz to 125 kHz and a resonance frequency (F_r) of 124.4 kHz. The connection between voltages of input and output is traditionally be represented by their ratio or gain. The output voltage is simply determined using in (1) after the input voltage V_i, gain M_g and turns ratio n are known [13]. Designing a converter for variable energy transfer and output voltage modification requires consideration of voltage transfer function. The characteristics of gain and its formula is described [14]-[16]. In (2) that represents an inductance ratio is used to combine two inductances into one. In (3) is provided below defines the quality factor "Q" in a resonant series circuit.

$$V_0 = M_g * \frac{1}{n} * \frac{V_i}{2} \quad (1)$$

$$L_n = \frac{L_m}{L_r} \quad (2)$$

$$Q = \frac{\sqrt{\frac{L_r}{C_r}}}{R_e} \quad (3)$$

The graph illustrates the relation between gain (M) and input voltage (V_i) over a range of n values from 15 to 19. Different values of n are represented by each line and as the input voltage increases the gain reduces, gain is highest at n=19 and lowest at n=15. The input voltage (V_i) between 370 and 410 volts is shown by the x-axis and gain (M) spans from 0.86 to 1.21 on the y-axis is represented in Figure 2 [17]. Figure 3 signifies the correlation between the magnetizing inductor (L_m) and the inductor ratio (L_n), magnetizing inductor (L_m) value elevates from 250 µH to 430 µH as the inductor ratio goes from 3.5 to 7, system inductance increases as the inductor ratio improves. Quality factor Q variation with respect to resistance in ohm (Ω) is observed in Figure 4. Obtaining the optimum values for Q, gain, n and L_n in order to enhance the power converter's performance is the aim of this paper. Thus, this paper offers comprehensive design computations and a controller comparison for the respective design, particularly between PIDD2 and PID, which is covered in section 3. The performance of an LLC resonant converter is critical on the size of the inductor as well as the values of gain, L_n and n. Achieving the intended output performance, controlling voltage, minimizing switching losses and maximizing power conversion efficiency are all made possible by carefully choosing these parameters. The resonant frequency is influenced by the size of the inductor, while the stability and operating range of the converter are determined by gain, L_n and n. L_n also has an impact on the transformer design, particularly the turns ratio, which has an impact on voltage isolation and scaling. In the converter, optimizing L_n aids in achieving a balance between size, cost and performance trade offs. The LLC converter gain establishes the connection between the input and output voltages. The converter can control the output voltage over a variety of input voltages and load circumstances by adjusting the gain. Selecting an appropriate gain ensures converter operates well throughout all kinds of operational circumstances. In order to balance efficiency, thermal performance and dynamic responsiveness in LLC resonant converters, it is crucial to choose these parameters as best as possible.

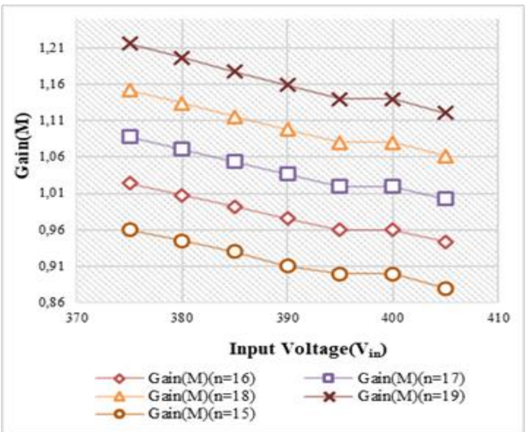

Figure 2. Deviation of input voltage based on gain (M)

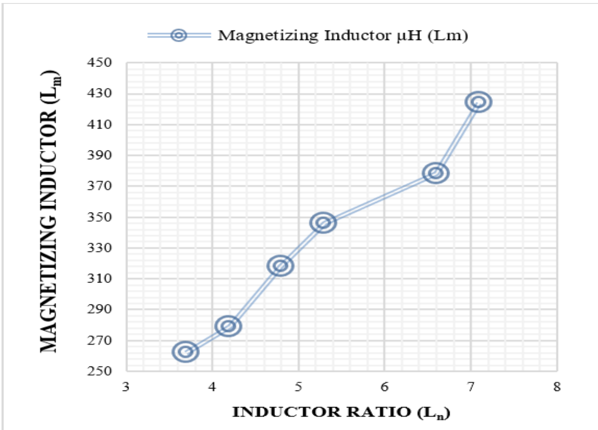

Figure 3. Variation of L_n pertaining to L_m

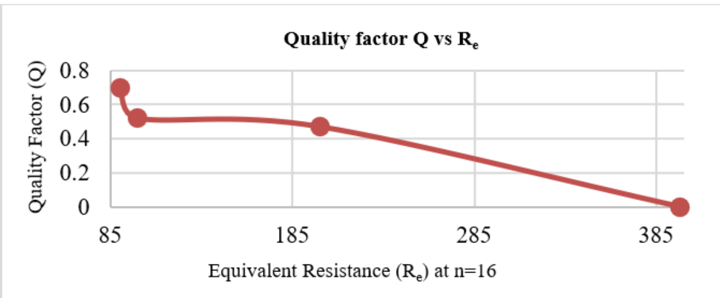

Figure 4. Variation of R_e with respect to Q

The extended describing function (EDF) technique is used to construct the gain, commonly known as input to output voltage transfer function [18]. A conventional small signal model of converters may be created using state space approximations to improvise the model accuracy for the LLC resonant converter, the small signal model that uses an EDF [19] has been considered in order to switch harmonics [20].

$$A = \begin{pmatrix} -1.542e^{11} & 1.665e^{6} & -1.667e^{4} & 0 & -110.1 & 110.1 & -110.1 & 110.1 \\ 4.758e^{5} & -4.758e^{5} & 0 & 3.205e^{-12} & 31.46 & -31.46 & 31.46 & -31.46 \\ 3.663e^{7} & 0 & 0 & 0 & 0 & 0 & 0 & 0 \\ 0 & 0 & 0 & -2.085e^{4} & -10 & -10 & -10 & -10 \\ 2.643e^{4} & -2.643e^{4} & 0 & -4000 & -5998 & 1998 & -1998 & -2002 \\ -2.643e^{4} & 2.643e^{4} & 0 & -4000 & 1998 & -5998 & -2002 & -1998 \\ 2.643e^{4} & -2.643e^{4} & 0 & -4000 & -1998 & -2002 & -5998 & 1998 \\ -2.643e^{4} & 2.643e^{4} & 0 & -4000 & -2002 & -1998 & 1998 & -5998 \end{pmatrix}$$

$$B = \begin{pmatrix} 1.667e^{4} \\ 0 \\ 0 \\ 0 \\ 0 \\ 0 \\ 0 \\ 0 \end{pmatrix}$$

$$C = (0\ 0\ 0\ 1\ 0\ 0\ 0\ 0)$$

$$D = (0)$$

$$\frac{dx}{dt} = A\hat{x} + B\hat{u}$$

$$\hat{y} = C\hat{x} + D\hat{u}$$

The following matrices represent state space of the LLC resonant converter: where, state-space system matrices are A, B, C, and D, $\hat{x}$ is state vector of the state space model, $\hat{u}$ is the control vector input, $\hat{y}$ is the vector output, the system transfer function is given by G as in (4).

$$G = \frac{-1.174e^{-6}s^{5} - 0.1335s^{4} - 1962s^{3} - 7.751e^{6}s^{2} - 1.063e^{6}s + 1.753e^{-7}}{s^{8} + 1.542e^{11}s^{7} + 8.026e^{16}s^{6} + 3.397e^{21}s^{5} + 5.149e^{25}s^{4} + 3.329e^{29}s^{3} + 7.837e^{32}s^{2} + 3.098e^{33}s - 1.936e^{21}} \quad (4)$$

3. COMPARISON OF PID AND PIDD2 CONTROLLER

This section presents two methods for controlling the voltage output of LLC resonant converters namely PID and PIDD2 controller. Preserving the actual voltage at the reference value is the controller's function. The difference between the reference and actual terminal voltage forms the error signal, which is created when the voltage at the converter is detected using the sensor. The control signal is produced by the controller based on the error signal, must pass through the PFM so as to allow the controller to modulate the frequency in terms of the input voltage. Additionally, the signal is a gate driver input that establishes the driving voltage for the converter's switches as represented in Figure 5.

3.1. Proportional integral derivative controller

Multiple architectures like series, parallel or hybrid are feasible. The most traditional parallel PID structure in this study is depicted in Figure 6 [21], [22]. The error signal e(t) is connected with control signal u(t) through PID controller in which K_p, $K_{i,}$ and K_d stands for the proportional gain, integral gain and derivative gain respectively, e(t) is the error signal and u(t) is the controller's output [23], [24], through Zeigler Nichols tuning procedure, the values of K_p, $K_{i,}$ and K_d are determined. The following is the expression as in (5) for its temporal description,

$$u(t) = K_p\, e(t) + K_i \int_0^t e(t')\, dt' + K_d \frac{de(t)}{dt} \quad (5)$$

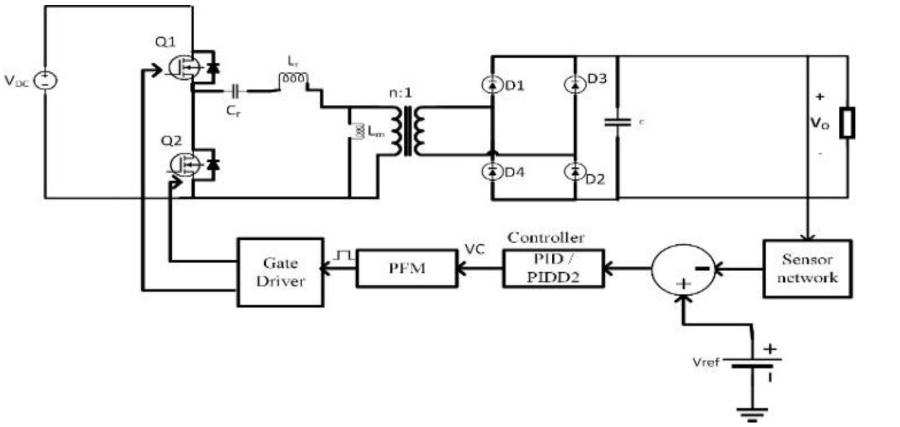

Figure 5. Controller representation with LLC resonant converter schematic

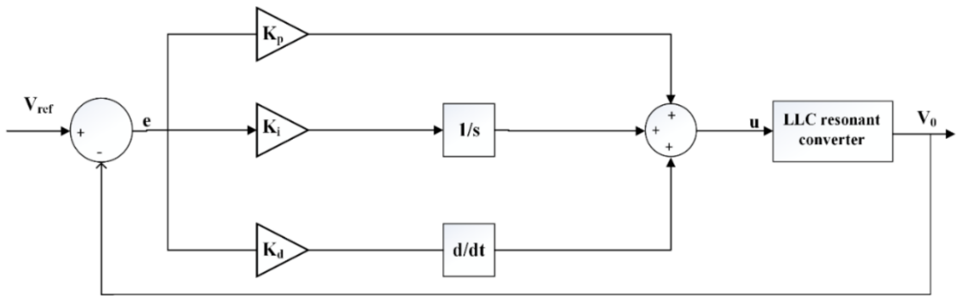

Figure 6. PID controller schematic

3.2. Proportional integral derivative double derivative

A popular version of controller PID is PIDD2 or PIDA or double derivative PID controller. It differs from conventional PID controllers by including a term of derivative of the second order and schematic PIDD2 is represented in Figure 7 [25]. It enhances the plant stability, accuracy in steady state and phase margin. Both the vibration inaccuracy caused by oscillation and the reaction settling time are decreased as a result. The controller PIDD2 is represented in its transfer function form as in (6) and practical form as in (7) as follows, where coefficient gains of PIDD2 are K_p, K_i, K_d, and K_a and its values are found using Zeigler Nichols tuning method.

$$G(s) = K_p + \frac{K_i}{s} + K_d s + K_a s^2 \tag{6}$$

$$G(s) = K_p + \frac{K_i}{s} + \frac{K_d s}{\tau s+1} + \frac{K_a s^2}{(\tau s+1)^2} \tag{7}$$

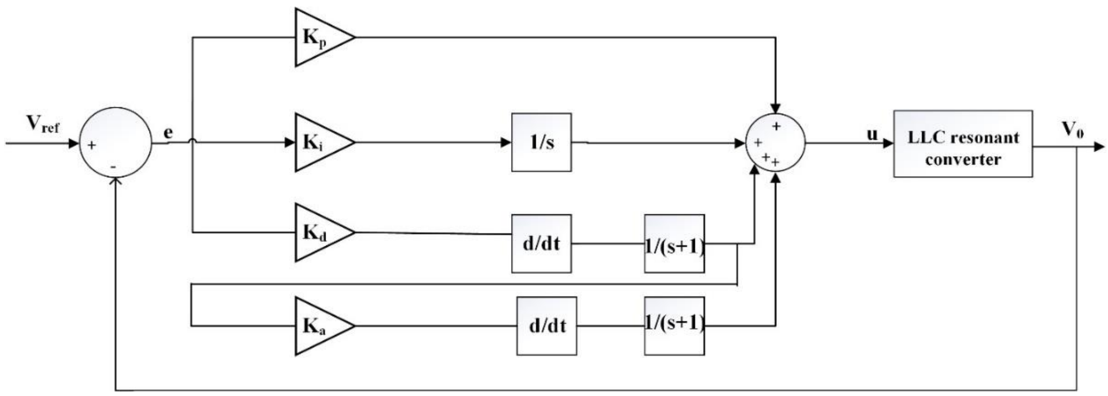

Figure 7. PIDD2 controller schematic

4. RESULTS AND DISCUSSION

Performance of the PIDD2 and PID controller with the above LLC resonant converter is simulated to demonstrate the effectiveness of modified controller as shown in Figures 8 and 9, the parameters of different components of the converter are considered as mentioned in Table 1. MATLAB/Simulink R2023a is used to conduct and discuss the simulation results. Controllers PIDD2 and PID in Simulink are used to construct closed loop control. Assessment is done using supply voltage disturbance for line variation and load resistance disturbance for load variation. According to the simulation results depicted in Figure 8, PIDD2 has enhanced the system's dynamic performance for both abrupt changes in load current and line voltage. The discussions are made below in sub sections.

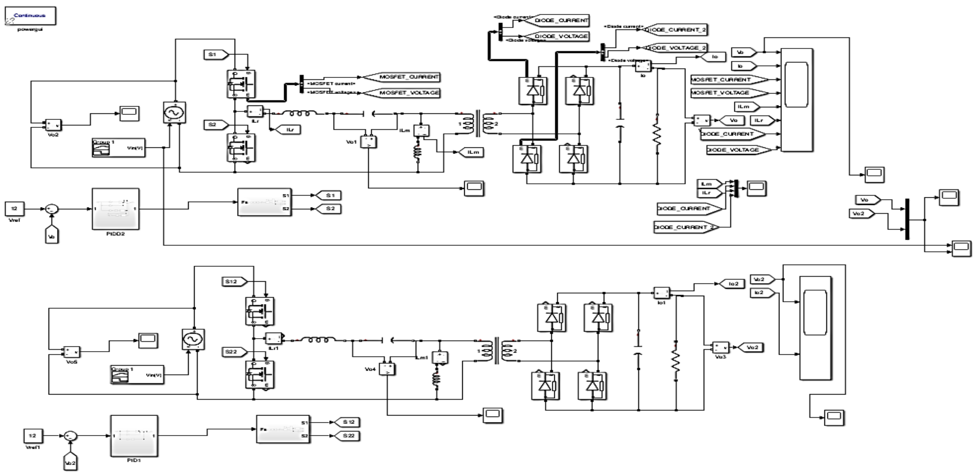

Figure 8. Simulink PIDD2 and PID control model with line variation

Table 1. The parameters of LLC resonant converter

S. No.	Parameters	Value
i	Input voltage, V_i	368V- 420V
ii	Output voltage, V_o	12V
iii	Output current, I_o	25A
iv	Resonant inductor, L_r	60 µH
v	Magnetizing inductor, L_m	210 µH
vi	Resonant capacitor, C_r	27.3 nF

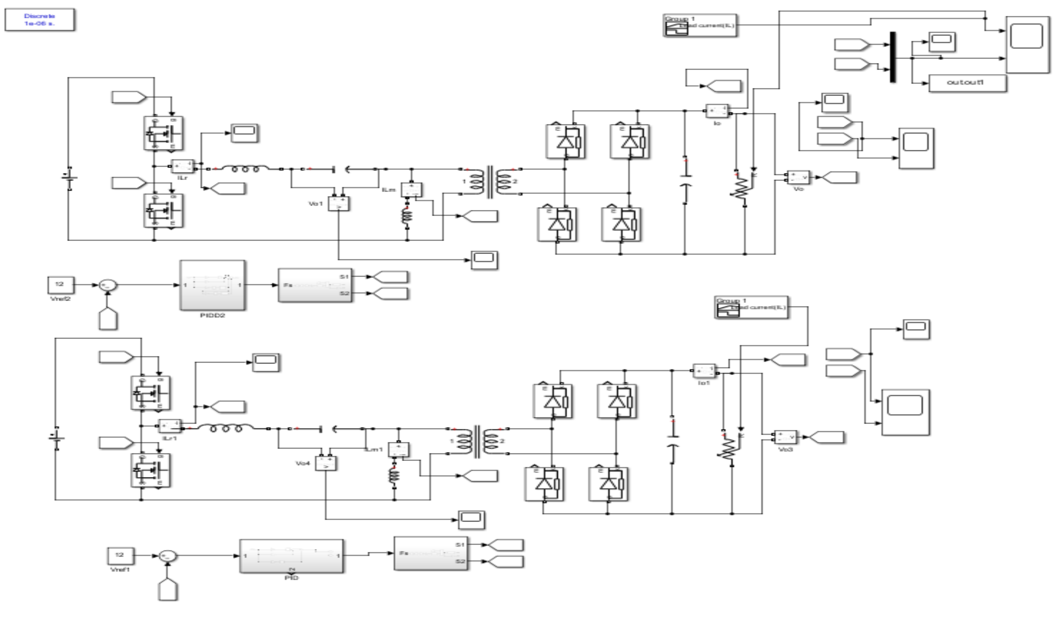

Figure 9. Simulink PIDD2 and PID control model with load variation

4.1. Case 1 with line variation

In this scenario, multiple fold analysis has been taken into consideration, where the input line voltage (V_i) varying between 368 V→380 V→360 V→400 V at t=0.022s, 0.05s, and 0.09s in simulation. Figure 10 demonstrates the converter V_o response with PIDD2 and PID controller in the presence of line variations. The suggested PIDD2 design control outperforms interms of faster response time and less overshoot than the traditional PID control approach in abrupt variations in V_i as can be shown from the Figure 10 and Table 2.

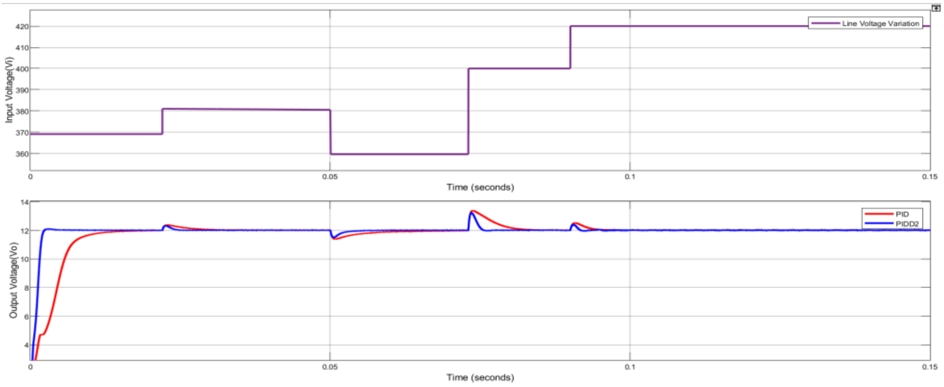

Figure 10. V_o response for voltage input changes

Table 2. The performance of PID and PIDD2 controllers with line variation

Method	PID controller	PIDD2 controller
Rise time (s)	3.34 ms	1.434 ms
Settling time (s)	2.14 ms	1.604 ms
Overshoot (%)	0.896	0.341

4.2. Case 2 with load change

At t=0.05 s, 0.075 s, 0.1 s and 0.1245 s respectively, the load varies as R_L=4.8 Ω→2.4Ω → 1.2 Ω →2.4 Ω→0.48 Ω in simulation. Figure 11 demonstrates the V_0 responses for the converter LLC with PIDD2 and PID controller in the presence of load variations. In the case of abrupt changes in load, the suggested PIDD2 control design outperforms with faster response time and less overshoot than the traditional PID control approach, according to Table 3 and Figure 11.

Table 3. The performance of PID and PIDD2 controllers with load variation

Method	PID controller	PIDD2 controller
Rise time (s)	1.372 ms	843.475 µs
Settling time (s)	3.051 ms	1.936 ms
Overshoot (%)	4.509	0.853

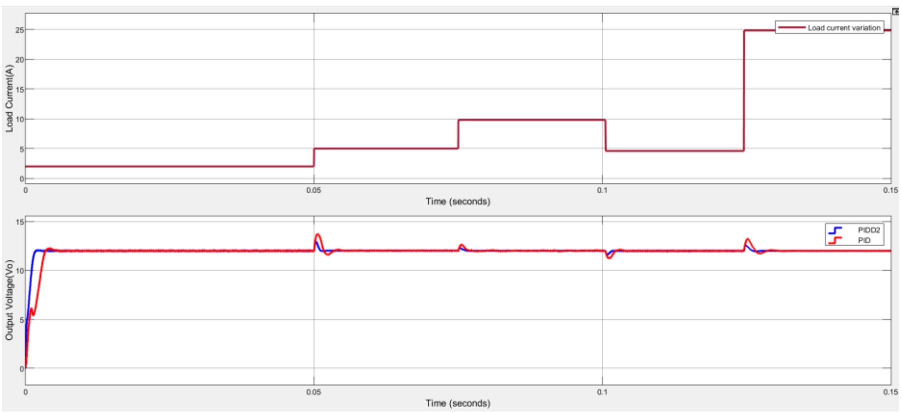

Figure 11. V_o response for sudden load change

5. CONCLUSION

The outcome of this paper provides several significant advances to the domain of power electronics and resonant converter control. This work demonstrates effective voltage regulation using modified PIDD2 over conventional PID controllers, particularly when used to LLC resonant converters. The voltage across output of LLC resonant converter is controlled using a PID and PIDD2 controller in the proposed work to reliably monitor the required value. Moreover, by substituting the PIDD2 controller for traditional control techniques, this paper gives a new perspective on control design approaches. MATLAB/Simulink simulations are used to validate design of controller. The findings contribute to the ongoing examination of control design specifically addressing challenges in attaining steady and effective performance in LLC resonant converters, the suggested PIDD2 controller outperforms the published PID control architecture. Furthermore, the thorough modelling and simulation work that has been given here can act as a starting point for additional investigation, motivating researchers to optimize control methods for increasingly intricate and demanding applications. The enhanced control accuracy and resilience has lead to increased efficiency and dependability across a range of high frequency power conversion applications, including telecommunications, electric cars, and renewable energy systems.

REFERENCES

[1] M. I. Shahzad, S. Iqbal, and S. Taib, “LLC series resonant converter with PID controller for battery charging application,” *in 2014 IEEE Conference on Energy Conversion (CENCON)*, Johor Bahru, Malaysia, Oct. 2014, pp. 84–89. doi: 10.1109/CENCON.2014.6967481.

[2] S. S. Shah, U. Raheja, and S. Bhattacharya, “Input Impedance Analyses of Charge Controlled and Frequency Controlled LLC Resonant Converter,” in *2018 IEEE Energy Conversion Congress and Exposition (ECCE)*, Portland, OR, USA: IEEE, Sep. 2018, pp. 1–5. doi: 10.1109/ECCE.2018.8558222.

[3] H. Kato *et al*., “Comparative analysis of full bridge and half bridge current resonant DC-DC converter,” in *2011 IEEE 33rd International Telecommunications Energy Conference (INTELEC)*, Amsterdam, Netherlands: IEEE, Oct. 2011, pp. 1–6. doi: 10.1109/INTLEC.2011.6099776.

[4] Z. Fang, J. Wang, S. Duan, K. Liu and T. Cai, “Control of an LLC resonant converter using load feedback linearization,” in *IEEE Transactions on Power Electronics*, vol. 33, no. 1, pp. 887-898, Jan. 2018, doi: 10.1109/TPEL.2017.2672731.

[5] X. Jin, X. Zhou, W. Wang, Z. Ma, J. Xu, and Z. Lu, “A half-bridge LLC converter for wide input voltage range applications,” in *2018 IEEE International Power Electronics and Application Conference and Exposition (PEAC)*, Shenzhen, Nov. 2018, pp. 1–5. doi: 10.1109/PEAC.2018.8590334.

[6] D. Ounnas, D. Guiza, Y. Soufi, R. Dhaouadi, and A. Bouden, “Design and implementation of a digital PID controller for DC–DC buck converter,” in *2019 1st International Conference on Sustainable Renewable Energy Systems and Applications (ICSRESA)*, Tebessa, Algeria, 2019, pp. 1–4. doi: 10.1109/ICSRESA49121.2019.9182430.

[7] Sathya K; Guruswamy K P, “Design and simulation of resonant LLC power converter for battery charging application,” *2023 International Conference on Electrical, Computer and Energy Technologies (ICECET)*, Cape Town, South Africa, 2023, doi: 10.1109/DELCON54057.2022.9753654.

[8] M. Kumar and Y. V. Hote, “Robust PIDD2 Controller Design for Perturbed Load Frequency Control of an Interconnected Time-Delayed Power Systems,” in I*EEE Transactions on Control Systems Technology*, vol. 29, no. 6, pp. 2662-2669, Nov. 2021, doi: 10.1109/TCST.2020.3043447.

[9] K. H. Ang, G. Chong and Yun Li, “PID control system analysis, design, and technology,” in *IEEE Transactions on Control Systems Technology*, vol. 13, no. 4, pp. 559-576, July 2005, doi: 10.1109/TCST.2005.847331

[10] S. Li and B. Fahimi, “State-space modelling of LLC resonant half-bridge DC–DC converter,” *IET Power Electron*., vol. 13, no. 8, pp. 1583–1592, Jun. 2020, doi: 10.1049/iet-pel.2019.1503.

[11] H. -N. Vu and W. Choi, “A Novel Dual Full-Bridge LLC Resonant Converter for CC and CV Charges of Batteries for Electric Vehicles,” in *IEEE Transactions on Industrial Electronics,* vol. 65, no. 3, pp. 2212-2225, March 2018, doi: 10.1109/TIE.2017.2739705.

[12] M. P. Foster, H. I. Sewell, C. M. Bingham, D. A. Stone, D. Hente and D. Howe, “Cyclic-averaging for high-speed analysis of resonant converters,” in *IEEE Transactions on Power Electronics*, vol. 18, no. 4, pp. 985-993, July 2003, doi: 10.1109/TPEL.2003.813763.

[13] R. A. Saleh and A. R. Newton, “The exploitation of latency and multirate behavior using nonlinear relaxation for circuit simulation,” in I*EEE Transactions on Computer-Aided Design of Integrated Circuits and Systems*, vol. 8, no. 12, pp. 1286-1298, Dec. 1989, doi: 10.1109/43.44509.

[14] H. Hu, X. Fang, F. Chen, Z. J. Shen and I. Batarseh, “A modified high-efficiency LLC converter with two transformers for wide input-voltage range applications,” in *IEEE Transactions on Power Electronics*, vol. 28, no. 4, pp. 1946-1960, April 2013, doi: 10.1109/TPEL.2012.2201959.

[15] Ming-Tzu Ho and Chia-Yi Lin, “PID controller design for robust performance,” in *IEEE Transactions on Automatic Control*, vol. 48, no. 8, pp. 1404-1409, Aug. 2003, doi: 10.1109/TAC.2003.815028.

[16] M. Javdan, “Transfer-function synthesis using PID controllers,” in *IEEE Transactions on Automatic Control*, vol. 23, no. 4, pp. 755-756, August 1978, doi: 10.1109/TAC.1978.1101816.

[17] L. A. D. Ta, N. D. Dao and D. -C. Lee, “High-efficiency hybrid LLC resonant converter for on-board chargers of plug-in electric vehicles,” in *IEEE Transactions on Power Electronics,* vol. 35, no. 8, pp. 8324-8334, Aug. 2020, doi: 10.1109/TPEL.2020.2968084.

[18] C. -H. Chang, E. -C. Chang, C. -A. Cheng, H. -L. Cheng and S. -C. Lin, “Small signal modeling of LLC resonant converters based on extended describing function,” *2012 International Symposium on Computer, Consumer and Control*, Taichung, Taiwan, 2012, pp. 365-368, doi: 10.1109/IS3C.2012.99.

[19] S. Tian, F. C. Lee and Q. Li, “A simplified equivalent circuit model of series resonant converter,” in *IEEE Transactions on Power Electronics*, vol. 31, no. 5, pp. 3922-3931, May 2016, doi: 10.1109/TPEL.2015.2464351.

[20] J. C. Basilio and S. R. Matos, "Design of PI and PID controllers with transient performance specification," in *IEEE Transactions on Education*, vol. 45, no. 4, pp. 364-370, Nov. 2002, doi: 10.1109/TE.2002.804399.
[21] M. Kumar and Y. V. Hote, "Real-time performance analysis of PIDD2 controller for nonlinear twin rotor TITO aerodynamical system," *Journal of Intelligent & Robotic Systems*, vol. 101, no. 3, p. 55, Mar. 2021, doi: 10.1007/s10846-021-01322-4.
[22] Qing-Guo Wang, Tong-Heng Lee, Ho-Wang Fung, Qiang Bi and Yu Zhang, "PID tuning for improved performance," in *IEEE Transactions on Control Systems Technology*, vol. 7, no. 4, pp. 457-465, July 1999, doi: 10.1109/87.772161.
[23] R. L. Steigerwald, "A comparison of half-bridge resonant converter topologies," in *IEEE Transactions on Power Electronics*, vol. 3, no. 2, pp. 174-182, April 1988, doi: 10.1109/63.4347.
[24] Y. Wei, Q. Luo, Z. Wang, A. Mantooth and X. Zhao, "Comparison between Different Analysis Methodologies for LLC Resonant Converter," *2019 IEEE Energy Conversion Congress and Exposition (ECCE)*, Baltimore, MD, USA, 2019, pp. 4429-4434, doi: 10.1109/ECCE.2019.8912840.
[25] S. Tian, F. C. Lee and Q. Li, "Equivalent circuit modeling of LLC resonant converter," *2016 IEEE Applied Power Electronics Conference and Exposition (APEC)*, Long Beach, CA, USA, 2016, pp. 1608-1615, doi: 10.1109/APEC.2016.7468082.

BIOGRAPHIES OF AUTHORS

Sathya K. received BE in electrical and electronics engineering (EEE) from DSCE, Bengaluru and M.Tech. in power electronics (PE) from BMS college of engineering, Bengaluru, Karnataka, India. She is currently pursuing Ph.D. in electrical engineering, UVCE, Bengaluru, India. She was associated as an assistant professor with Cambridge Institute of Technology (CITech), Bengaluru from 2018 to 2022, in Dept. of EEE. Her current research interests include design of power converters, DC-DC converters, resonant converters, electric vehicles, and optimization. She can be contacted at email: sathya.k@uvce.ac.in.

Dr. K. P. Guruswamy is an associate professor, department of electrical engineering, UVCE, Bengaluru, Karnataka, India. He obtained his BE and ME in electrical engineering from UVCE, Bengaluru. He was awarded Ph.D. in electrical engineering from IIT Roorkee. His vast experience and expertise in the field of modeling of power converters, digital control of converters and resonant converters. He can be contacted at email: guruswamykp@uvce.ac.in.